



Contents lists available at ScienceDirect

Medical Engineering & Physics

journal homepage: www.elsevier.com/locate/medengphy



Maximum Lyapunov exponents as predictors of global gait stability: A modelling approach

Sjoerd M. Bruijn^{a,b,*}, Daan J.J. Bregman^c, Onno G. Meijer^{b,d,e}, Peter J. Beek^b, Jaap H. van Dieën^b

^a Motor Control Laboratory, Research Center for Movement Control and Neuroplasticity, Dep. of Biomedical Kinesiology, K.U. Leuven, Belgium

^b Research Institute MOVE, Faculty of Human Movement Sciences, VU University, Amsterdam, The Netherlands

^c Research Institute MOVE, VU University Medical Center, Dept. Rehabilitation Medicine, Amsterdam, The Netherlands

^d Second Affiliated Hospital of Fujian Medical University, Zhongshan Northern Road 34, Quanzhou 362000, Fujian, PR China

^e Department of Rehabilitation, Fujian Medical University, Fuzhou, Fujian, PR China

ARTICLE INFO

Article history:

Received 16 December 2010

Received in revised form 28 July 2011

Accepted 28 July 2011

Keywords:

Biomechanics

Gait stability

Lyapunov exponents

Passive dynamic walking

Modelling

Locomotion

ABSTRACT

To examine the stability of human walking, methods such as local dynamic stability have been adopted from dynamical systems theory. Local dynamic stability is calculated by estimating maximal finite time Lyapunov exponents (λ_S and λ_L), which quantify how a system responds continuously to very small (i.e. “local”) perturbations. However, it is unknown if, and to what extent, these measures are correlated to global stability, defined operationally as the probability of falling.

We studied whether changes in probability of falling of a simple model of human walking (a so-called dynamic walker) could be predicted from maximum finite time Lyapunov exponents. We used an extended version of the simplest walking model with arched feet and a hip spring. This allowed us to change the probability of falling of the model by changing either the foot radius, the slope at which the model walks, the stiffness of the hip spring, or a combination of these factors.

Results showed that λ_S correlated fairly well with global stability, although this relationship was dependent upon differences in the distance between initial nearest neighbours on the divergence curve. A measure independent of such changes (the log(distance between initially nearest neighbours after 50 samples)) correlated better with global stability, and, more importantly, showed a more consistent relationship across conditions. In contrast, λ_L showed either weak correlations, or correlations opposite to expected, thus casting doubt on the use of this measure as a predictor of global gait stability.

Our findings support the use of λ_S , but not of λ_L , as measure of human gait stability.

© 2011 IPEM. Published by Elsevier Ltd. All rights reserved.

1. Introduction

With their high incidence and associated costs, falls form a considerable problem in modern society [1]. Consequently, there is a rapidly growing body of research focusing on falls and the stability of walking and standing in the elderly [2–5], as well as various patient groups prone to have problems in standing and walking, such as patients with osteoarthritis [6], anterior cruciate ligament ruptures [7], peripheral neuropathy [8,9] and amputees [10].

To study the stability during walking, methods such as local dynamic stability have been adopted from dynamical systems theory [11,12]. Local dynamic stability is calculated by estimating maximal finite time Lyapunov exponents (λ_S and λ_L , capturing short (λ_S) and longer term (λ_L) responses, respectively), which

quantify how a system responds continuously to very small (i.e. “local”) perturbations [6,7,13–18]. λ_S and λ_L indicate the rate of divergence of neighbouring trajectories in state space; values of $\lambda < 0$ indicate a stable system, with neighbouring trajectories tending to move closer together after some time; values of $\lambda > 0$ indicate an unstable system, with neighbouring trajectories tending to diverge from each other. Higher values of λ indicate less stable systems.

Maximum finite time Lyapunov exponents have a sound mathematical foundation [12] and have been used for almost a decade now to quantify human gait stability, for example by comparing patients to healthy controls, or by comparing younger to elderly subjects [2,7,9,11,19,20,17,21,22]. Several algorithms exist for calculating maximum finite time Lyapunov exponents, but Rosenstein's algorithm [12] is used most often in analysing gait data. As the different algorithms may lead to slightly different results, it is of importance to consider the results of a given study in the light of the algorithm used. In the current paper, we only mention when studies used another algorithm than Rosenstein's.

* Corresponding author at: Motor Control Laboratory, Research Center for Movement Control and Neuroplasticity, Dep. of Biomedical Kinesiology, K.U. Leuven, Tervuursevest 101, 3001 Leuven, Belgium. Tel.: +32 483404701.

E-mail address: s.m.bruijn@gmail.com (S.M. Bruijn).

While there is little doubt that maximum finite time Lyapunov exponents capture a system's response to very small, local perturbations [8,11], it is unknown if, and to what extent, they relate to common sense notions of stability, such as the probability of falling [9,11,14–16,23]. When assuming that patients and elderly have a higher chance of falling, the notion that maximum finite time Lyapunov exponents reflect a higher chance of falling is supported by several studies on these subject groups [2,7,9,11,19,20,17,21,22]. However, this assumption is not straightforward because patients and elderly may adapt their gait, such that stability may even be increased [24,25].

Another approach to reveal whether maximum finite time Lyapunov exponents relate to the probability of falling is to study whether subjects with reported balance problems display higher maximum finite time Lyapunov exponents. Lockhart and Liu [2] applied this method, and reported greater maximum finite time Lyapunov exponents (particularly λ_S) in elderly subjects who fell after an experimentally induced slip compared to elderly subjects who did not. However, in the study by Lockhart and Liu [2] walking speed was different between groups, which may be a confounder when studying stability [14]. In a recent study on knee osteoarthritis in which walking speed was controlled for, no relationship between self reported number of falls and maximum finite time Lyapunov exponents was found [6]. Still, in other studies, in which subjects' gait stability was reduced experimentally by either having them walk over a compliant surface [26], by applying randomly varying galvanic stimulation [27], or by mechanical and visual perturbations [28], the reduction in stability could be demonstrated using λ_S , although λ_L suggested that subjects were actually walking more stable. This latter finding has been attributed to the different time scales on which the two measures operate: in the short term, walking may be less stable, but adaptations have been suggested to make the gait pattern more stable in the long term [6].

In another attempt to unravel the relationship between local dynamic stability and probability of falling in gait, Su and Dingwell [29] used a simple passive dynamic model, walking down a slope [30]. The probability of falling was gradually increased by alterations in the bumpiness of the slope. The simulation results indicated that λ_S increased linearly, while λ_L did not change with increasing bumpiness. Kurz et al. [31] performed a simulation study in which the walking model was propelled by power generated at the ankle. By gradually increasing the push-off noise at the ankle (which is equivalent to the noise in the slope in [30]), they found λ_S to increase, whereas the maximum perturbation that could be dealt with decreased (the perturbation was modelled as an instantaneous horizontal force, applied to the stance leg at mid-stance). A more recent study expanded these findings in a 3D walking model, showing that like for the other models, λ_S was predictive of fall risk in such a model, while λ_L was not [32]. These findings support the idea that λ_S is related to the probability of falling, but at the same time illustrate that the relationship between λ_L and probability of falling remains unclear.

It also remains unclear to what extent the results of the above-mentioned modelling studies [29,31,32] can be generalized; in all three studies the probability of falling was modified by adding external noise to either the slope (i.e. the bumpiness) [29], ankle push-off force [31], or the controller [32]. When comparing different groups of human subjects, however, it seems likely that they differ in more than just the variations in the level of noise in their control. For instance, it is well known that elderly and patients have a reduced ability to generate muscle force [33], and may show an altered gait coordination [34,35]. Moreover, subjects may differ in morphology (mass, mass distribution, height and leg length), which could also affect their stability. To date, it is unknown if maximum finite time Lyapunov exponents can predict the changes in probability of falling caused by changes in morphology, gait pattern,

or strength. If they are unable to do so even in a simple model of walking, this would render them less useful in assessing human gait stability.

In the present study, we examined whether changes in probability of falling of a passive dynamic walking model can be predicted from maximum finite time Lyapunov exponents. We used an extended version of the simplest walking model with arced feet and a hip spring [36]. We changed the probability of falling of the model by changing either the foot radius, the slope at which the model walks, the stiffness of the hip spring, or a combination of these factors. Adding a small amount of noise to the slope the model walked on allowed for natural variation in the trajectories, needed to calculate maximum finite time Lyapunov exponents.

2. Methods

2.1. General approach

We simulated walking using a simple passive dynamic walking model (for details, see Fig. 1, and the section “model” below), walking down a slope with different foot radii, slope angles, and hip stiffness values. For each model configuration, we searched for a stable walking solution, and subsequently determined the maximum perturbation the model could handle by having it perform steps down and steps up. In these trials, the model started from the stable solution, and only the first step was perturbed, by a floor height difference (either up or down), after which a maximum of 30 steps was simulated. The size of these perturbations was increased in steps of 0.00001 m, and the maximum step up or down was designated as the level at which the model could no longer walk 30 steps after the perturbation. The difference between maximum step up and step down was then designated as maximum perturbation (Maxpert [36]). Note that the maximum perturbation a model can handle is closely related to the probability of falling for a given noise level of the slope; the smaller the maximum perturbation, the more likely that a perturbation larger than this size will be encountered.

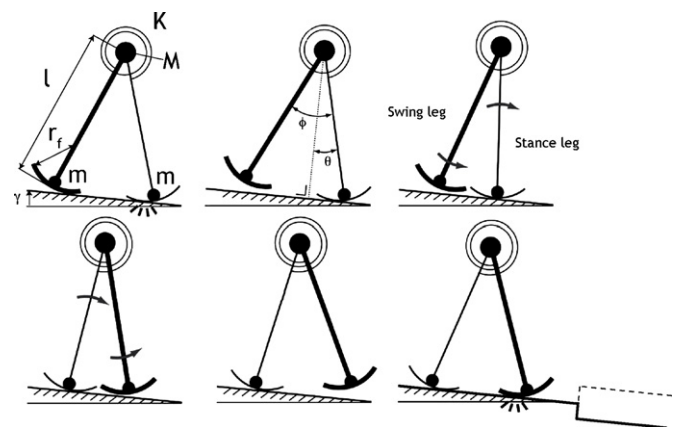


Fig. 1. A schematic representation of the model used. The model parameters are: leg length (l), foot radius (r_f), hip mass (M), foot mass (m), hip spring stiffness (k), gravitational acceleration (g), and slope angle (γ). Due to the normalization of the model ($M=1$, $l=1$, $g=1$), and while ignoring the infinitesimally small foot masses (i.e. $m \approx 0$), the only free model parameters are γ , k , and r_f . For a typical walking step, after foot-strike, the swing leg (heavy line) swings forward past the stance leg (thin line) until the swing leg hits the ground and a new step begins. θ is the angle between the stance leg and the slope normal, and φ the angle between the two legs. In the last figure, an example of a step up (dotted line) and step down are depicted. For the determination of the maximum perturbation, there was only one such perturbation, after which the floor level stayed equal. For the actual walking trials, each step would be perturbed by a change in floor height. Adapted from Garcia et al.

Next, for each configuration, 10 simulations of 200 steps were performed, with each simulation starting from the same stable solution. Bumpiness in the slope was modelled by adding a random term to the foot strike condition (see model details below). From the time series generated by these simulations, local dynamic stability was calculated (details below) and correlated to the maximum perturbation the model could handle.

2.2. The model

The forward-dynamic simulation model was based on previous walking models [30,36,37]. As can be seen in Fig. 1, the model comprised two legs with a negligible point mass at the feet, and a substantial point mass at the hip. The hip was modelled as a frictionless hinge joint. The massless feet were designed as perfect arcs, of which the radius could be adapted. The equations of motion of this system were obtained from [36]. The equations of motion were numerically integrated using an ODEsolver in Matlab (The Mathworks, Natick, MA).

We added noise to the model by modifying the height at which foot strike occurs [29]. During unperturbed walking, foot strike occurred when the swing foot reached a height of $h = 0$ (as the slope was modelled by placing the vector of gravity not exactly vertical), and was in front of the stance leg (i.e. $\theta < 0$). Instead of having $h = 0$, in our simulations, we set

$$h = c * n \quad (1)$$

with n being a random number, drawn from a normal distribution, and c representing a constant. Based on pilot experiments, we chose c to be 0.00001 m such that the model could still walk at all manipulations. This procedure ensured that there was sufficient variability in the trajectories of the model to calculate maximum finite time Lyapunov exponents.

2.2.1. Manipulations

For all manipulations, the model started with a foot radius of 0 m, a hip stiffness 0 N m/rad, and a slope angle of 0.04 rad. From this starting configuration, we used four different manipulations to the model:

1. Foot radius was increased from 0 m in steps of 0.05 m until the model could no longer walk (0.9 m). In this manipulation, step length increased with increasing foot radius.
2. As the previous manipulation, except that in this case the slope was adjusted so that step length did not increase.
3. Hip stiffness was increased in steps of 0.5 N m/rad to a maximum of 10 N m/rad. In this manipulation, step length decreased with increasing hip stiffness.
4. As the previous manipulation, except that in this case the slope was adjusted so that step length did not decrease.

2.2.2. Calculation of maximum finite time Lyapunov exponents

The time series of the four state variables of the model, obtained from the simulations were first time-normalized to time series of 100 strides (200 steps) consisting of 10,000 data points each [14,38]. Then, these time series were used to construct state spaces for the calculation of the maximum finite time Lyapunov exponents, which, in accordance with the literature [11], and following Rosenstein's algorithm [12], were calculated as the slope of the logarithmic divergence curve. Specifically, λ_S and λ_L were calculated as the slopes of the $\log(\text{divergence})$ curves for 0–0.5 and 4–10 strides, respectively.

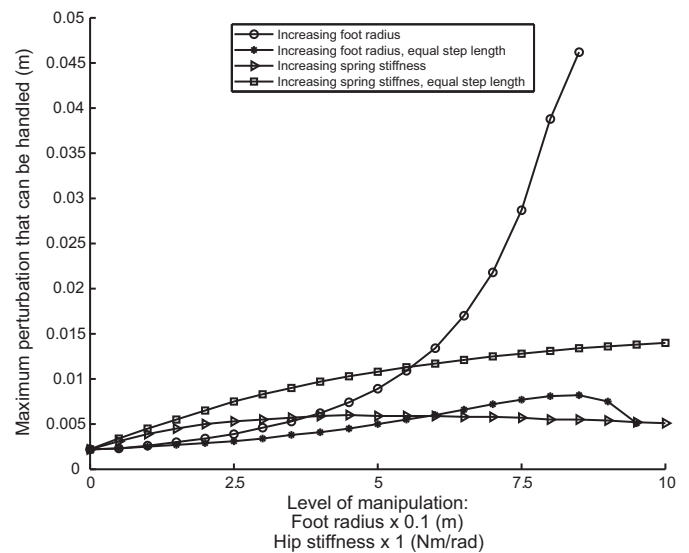


Fig. 2. Maximum perturbation (m) the model could handle under different manipulations (shown in different symbols). Note the different scaling factors for the different manipulations on the x-axis.

3. Results

3.1. Global stability at different manipulations

Fig. 2 shows the maximum perturbation (Maxpert) the model could handle under the four manipulations, illustrating that increased foot radius, hip stiffness and step length all yield higher global stability.

3.2. Relationships between measures

3.2.1. Short term maximum finite time Lyapunov exponent and maximum perturbation

Fig. 3 shows the relationship between λ_S and the maximum perturbation the model could handle for each manipulation. Because of differences in the range of the variables (theoretically, Maxpert has a range of $[0, \infty]$ while λ_S has a theoretical range of $[-\infty, \infty]$), λ_S was plotted vs. $\log(\text{Maxpert})$, to obtain a linear relationship. Although a

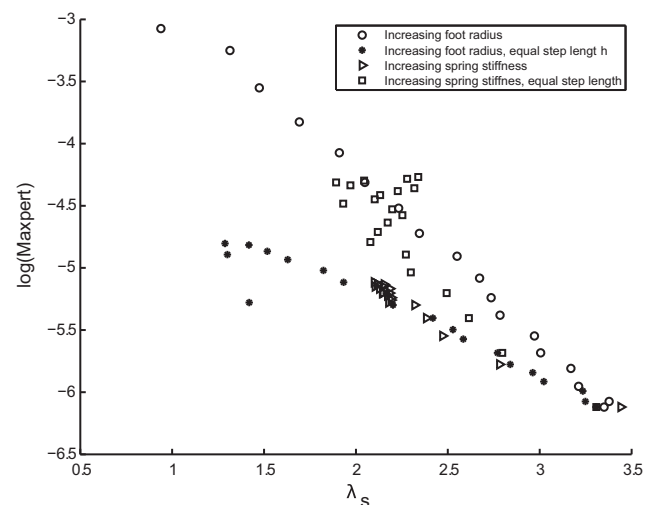


Fig. 3. Relationship between the log of the maximum perturbation the model could handle ($\log(\text{Maxpert})$), and λ_S for the different manipulations (which are shown in different symbols). Note that we plotted $\log(\text{Maxpert})$ instead of Maxpert on the y-axis in view of the observed non-linear relationship between Maxpert and λ_S .

Table 1
Relationships between the log of the maximum perturbation the model could handle ($\log(\text{Maxpert})$) and λ_S : The first column reports the regression coefficients (b), the second column the standard error of the regression coefficients ($\text{SE}(b)$), and the third column the correlation coefficients, while the last column indicates which regression coefficients were significantly different from each other (t -test, $P < 0.01$).

		λ_S			
		<i>B</i>	<i>SE(B)</i>	<i>R</i>	Different from
1	Manipulation of foot radius	−0.7471	0.0151	−0.9968	2,4
2	Manipulation of foot radius, equal step length	−1.5246	0.0953	−0.9666	1,3
3	Manipulation of hip spring stiffness	−0.5483	0.072	−0.868	2,4
4	Manipulation of hip spring stiffness, equal step length	−1.2306	0.056	−0.9809	1,3
Overall correlation				−0.786	

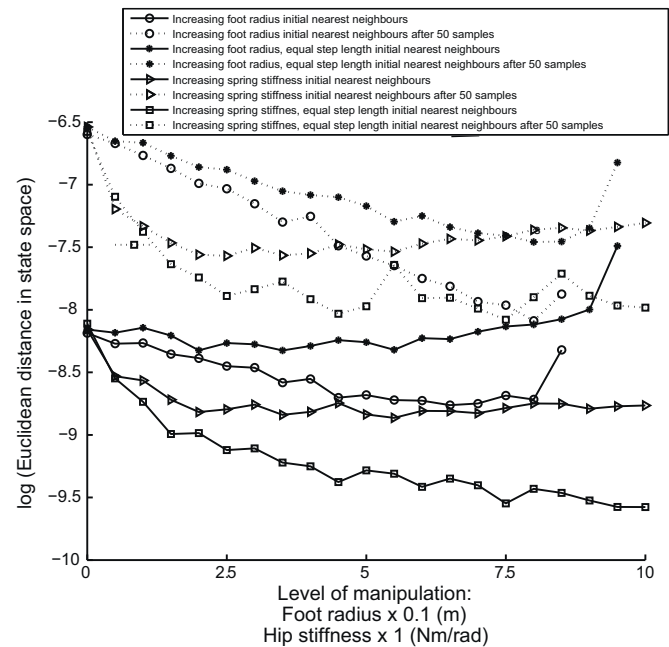


Fig. 4. Average $\log(\text{distance between initial nearest neighbours})$ (solid lines) and the average $\log(\text{distance between initial nearest neighbours after 50 samples})$ (dotted lines), for each manipulation (indicated by the symbols). Note the different scaling factors for the different manipulations on the x-axis. In this figure, the difference between solid and dotted lines represents a rough estimate of the slope of the divergence curve between 0 and 0.5 strides.

linear relationship was found within each manipulation, relationships were different for the different manipulations to the model, as is also apparent in the differences between regression coefficients for different manipulations (see Table 1).

In order to further explore why these differences may have arisen, we studied the range of the average logarithmic divergence curves from which λ_S was calculated in more detail. In Fig. 4, we plotted the average $\log(\text{distance between initial nearest neighbours})$ (solid lines), and average $\log(\text{distance between initial nearest neighbours after 50 samples})$ (dotted lines), for each manip-

Table 2
Relationships between the log of the maximum perturbation the model could handle ($\log(\text{Maxpert})$) and $\log(\text{distance between initial nearest neighbours at 50 samples})$: The first column reports the regression coefficients (b), the second column the standard error of the regression coefficients ($\text{SE}(b)$), and the third column the correlation coefficients. The last column indicates which regression coefficients were significantly different from each other (t -test, $P < 0.01$).

		$\log(\text{distance between initial nearest neighbours after 50 samples})$			
		<i>B</i>	<i>SE(B)</i>	<i>R</i>	Different from
1	Manipulation of foot radius	−0.4733	0.0317	−0.966	
2	Manipulation of foot radius, equal step length	−0.622	0.0475	−0.9513	
3	Manipulation of hip spring stiffness	−0.625	0.0714	−0.8952	
4	Manipulation of hip spring stiffness, equal step length	−0.7688	0.1019	−0.8659	
Overall correlation				−0.8854	

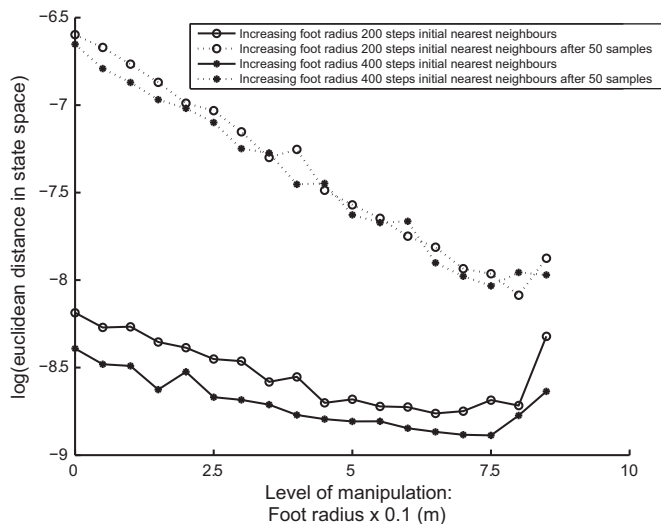


Fig. 6. Average log(distance between initial nearest neighbours) (solid lines) and the average log(distance between initial nearest neighbours after 50 samples) (dotted lines), as a function of the manipulation of foot radius, for different time series lengths. In this figure, the difference between solid and dotted lines represents a rough estimate of the slope of the divergence curve between 0 and 0.5 strides.

Table 2) than between maximum perturbation and λ_S . More importantly, regression coefficients were no longer different between manipulations. This strongly suggests a dependence of λ_S on the distance between initial nearest neighbours.

In earlier work, we proposed that decreases in the distance between initial nearest neighbours could be one of the mechanisms responsible for the increase in λ_S when using longer time-series (Bruijn et al., 2009). When more samples are present in the state space, the minimal distance between these samples decreases (i.e. when number of samples goes to infinity, the minimal distance goes to 0). In order to further investigate this dependency of λ_S on time-series length (and possibly, on log(distance between initial nearest neighbours)), we performed another set of simulations, this time only for changing foot radius, but now with 400 steps. The results of these simulations are shown in Fig. 6. As can be appreciated from this figure, the log(distance between initial nearest neighbours) clearly decreased when including more steps in the analysis, although there was almost no difference in log(distance between initial nearest neighbours after 50 samples), causing a clear increase in λ_S when using longer time-series.

3.2.2. Long term maximum finite time Lyapunov exponent and maximum perturbation

Fig. 7 shows the relationship between λ_L and the log(maximum perturbation) for each manipulation. As can be appreciated from this figure, the relationship between λ_L and the maximum perturbation was opposite to the expected relationship; higher values of λ_L seemed to coincide with higher stability. Moreover, as can be seen from Table 3, correlations for most manipulations, as well as over manipulations were relatively poor. Like λ_S , we further explored λ_L in terms of the region of the logarithmic divergence from which it was calculated in Fig. 8; from this figure it is apparent that: (1) while log(distance between initial nearest neighbours after 400 samples) is higher than log(distance between initial nearest neighbours after 50 samples), the patterns (across different manipulations) are still similar; (2) divergence hardly increases between 400 and 1000 samples; (3) the amount of divergence does not seem to be dependent on the distance between initial nearest neighbours after 400 samples, indicating that the maximum distance that can be reached in the attractor has not yet been reached for any of the curves.

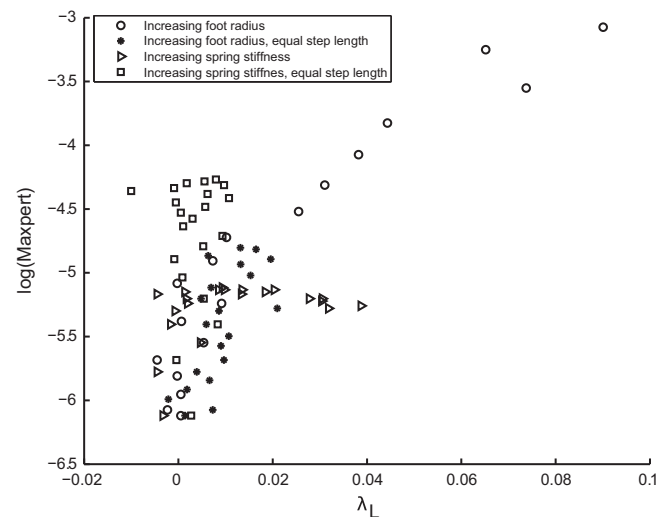


Fig. 7. Relationship between the log of the maximum perturbation the model could handle (log(Maxpert)), and λ_L for the different manipulations (which are shown in different symbols). Note that we plotted log(Maxpert) instead of Maxpert on the y-axis because of the observed non-linear relationship between Maxpert and λ_L .

4. Discussion and conclusion

In line with previous studies, the results of the present study suggest that λ_S relates to the probability of falling in a passive dynamic model [29,31,32], also when the instabilities are caused by factors other than noise. However, in contrast to previous simulations [29] we found a relationship that was either weak or opposite to expected between λ_L and the probability of falling in our model, with higher values of λ_L coinciding with higher maximum perturbation levels.

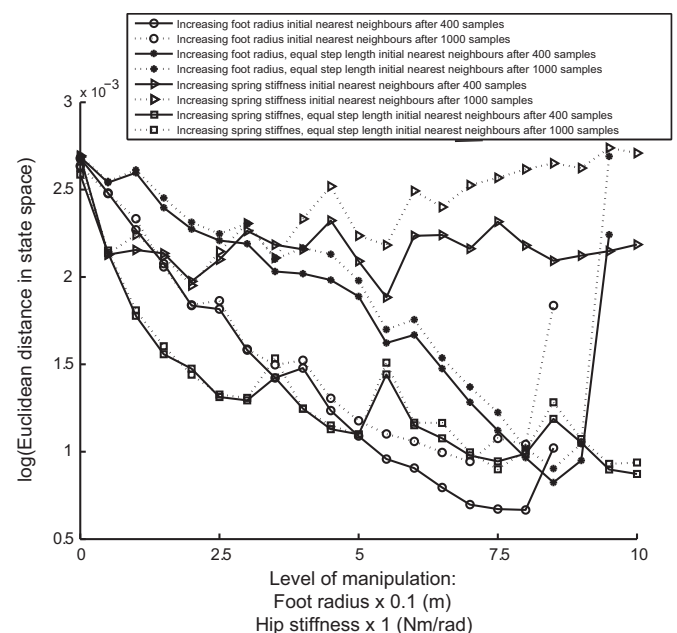


Fig. 8. Average log(distance between initial nearest neighbours after 400 samples) (solid lines), and the average log(distance between initial nearest neighbours after 1000 samples) (dotted lines), for each manipulation (indicated by the symbols). Note the different scaling factors for the different manipulations on the x-axis. In this figure, the difference between solid and dotted lines represents a rough estimate of the slope of the divergence curve between 4 and 10 strides.

Table 3
Relationships between the log of the maximum perturbation the model could handle (log(Maxpert)) and λ_1 : The first column reports the regression coefficients (b), the second column the standard error of regression coefficients (SE(b)), and the third column the correlation coefficients. The last column indicates which regression coefficients were significantly different from each other (t-test, $P < 0.01$).

		λ_L			
		B	SE(B)	R	Different from
1	Manipulation of foot radius	0.0278	0.0026	0.9344	2,3
2	Manipulation of foot radius, equal step length	0.0091	0.0024	0.6751	1
3	Manipulation of hip spring stiffness	0.0004	0.0022	0.0401	1
4	Manipulation of hip spring stiffness, equal step length	0.021	0.0116	0.3841	
Overall correlation				0.5941	

4.1. Relationship between λ_S and probability of falling

The observed relationship between λ_S and global stability (as expressed by the maximum allowable perturbation) was in agreement with and extends other studies on passive and powered dynamic walking models [29,31,32]. In other modelling studies, the main manipulation to such models was the noise in the model, whereas our main interest was in manipulating model parameters other than noise. Even for manipulations other than noise, λ_S predicted global stability fairly well. It should be mentioned that we also explored the effects of noise level (see Fig. 9), and found effects that were in accordance with the literature [29,31,32], while keeping the results of the model parameter manipulations the same.

To the best of our knowledge, there are very few studies showing that a pathological condition, or experimentally decreased stability, causes a decrease in λ_S . One example is a study [7] that reported lower values of λ_S in subjects with anterior crucament ligament (ACL) deficiencies. These authors regarded the lower λ_S as a sign of decreased complexity of movement, and, indeed, it could well be that the deficient ACL leads to an overcompensation behaviour which actually makes the knee more stable.

Our results showed an undesired dependency of λ_S on log(distance between initial nearest neighbours), which led to dif-

ferent relationships between λ_S and maximum perturbation for different manipulations. Moreover, this dependency might also explain previously reported increases in λ_S with increasing time-series length (i.e. with increasing time-series length more data points are available in the state space, and nearest neighbours are likely to be closer). Other reasons why nearest neighbours may be closer include:

- 1) An increased sampling frequency or reduced stride time—single revolutions along a trajectory contain more data points, leading to nearest neighbours laying closer together because phase shifts will be smaller.
- 2) A decrease in attractor size—lower speeds or angles make that consecutive data points lay closer together. This also makes that if initial nearest neighbours are in part separated by a phase shift, the distance caused by this phase shift will be smaller.
- 3) A decreased stride time variability—nearest neighbours are more likely to be more in the same phase of the stride cycle, thus reducing the distance caused by the phase shift.

Of course, the above-motioned factors interact, which hampers identifying their separate contributions. In our study, the first of the above points (i.e. change in sample rate or number of data points per revolution) likely played no role, as time series were normalized so that on average stride cycles contained the same number of samples, as has been recommended before in the literature [14,15,38]. The second point may be of greater importance. Of course, the attractor can be normalized so that the maximum distance within it is equal between different conditions. However, this would not alter the signal to noise ratio, and hence, problems due to differences in initial nearest neighbours would remain. The third point could be solved by normalizing stride cycles so that they have exactly the same length, as was suggested by England and Granata [38]. However, this may discard temporal variability, which can contain useful information on divergence along the trajectory.

An alternative solution to deal with the changes in distance between initial nearest neighbours comes from Zeng et al. [39], who proposed to look for nearest neighbours in a shell rather than a sphere (i.e. restricting both the maximum distance a nearest neighbour can have (as for a sphere), and the minimum distance it can have). In doing so, the changes in distance between initial nearest neighbours will be restricted to the ‘thickness’ of the shell, and the above problems may be overcome. However, this would introduce the problem of selecting a proper inner and outer radius for the shell, which depends on the data set under investigation, and consequently allows for different inner and outer shell radii between different experimental conditions and/or subgroups.

Another, theoretically less sound, yet practical way to overcome the problem of changes in log(distance between initial nearest neighbours) is to assume that all changes in log(distance between initial nearest neighbours) are due to differences in sampling noise. Changes in sampling noise will have less influence on the diver-

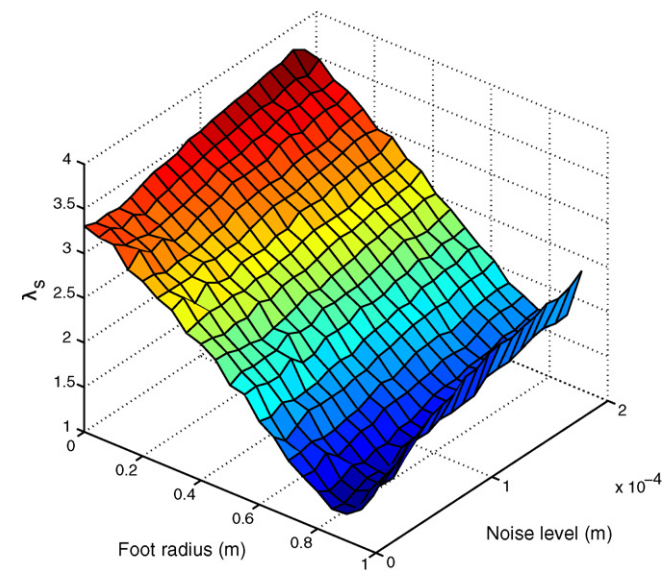


Fig. 9. The effects of noise level on the relationship between parameter manipulations and λ_S for the manipulation of foot radius with equal step length. As in previous studies, increasing noise levels (for the same parameter value) caused an increase in λ_S , indicating that the model was more likely to fall at that noise level. Still, similar effects of parameter values can be seen for each noise level, indicating the fact that the model configuration is still a determinant for how well the model can handle that noise level.

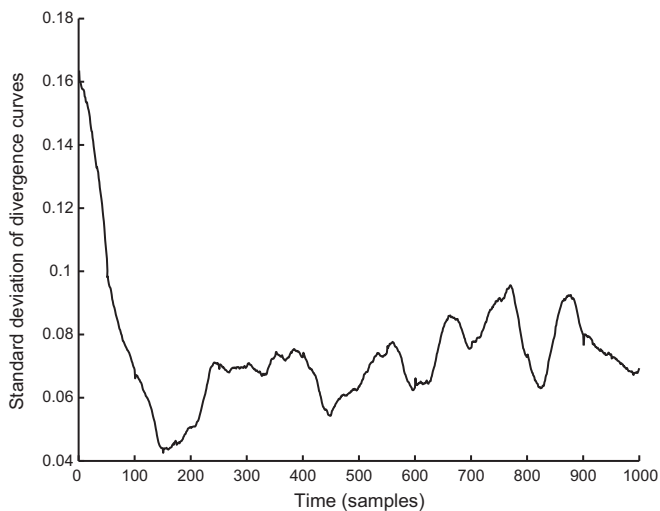


Fig. 10. Standard deviation of 10 divergence curves for one manipulation.

gence after some period of time when the system dynamics has become prominent. This can also be seen in Fig. 10, where we have plotted the standard deviation of the divergence curves generated from one manipulation; initially, standard deviations are high, but they quickly decrease. If we assume that all initial distances are equal (and changes therein are only a reflection of changes in sampling error), λ_S appears to be strongly related to the value of the divergence curve at any given moment. Indeed, our analysis using this method (see Table 2) yielded better results than our analysis of λ_S . Note that applying this method also decreases the variability of estimates of local dynamic stability, as the value of the divergence curve at 50 samples is less variable than the slope (which is also influenced by the variability in all samples up to 50).

In line with our findings, a recent study, which investigated the influence of visual and mechanical perturbations on the local dynamic stability of human gait, showed both higher values of λ_S and a higher value of the divergence curve overall in the presence of perturbations [28]. The present results indicate that global stability may depend more on the absolute divergence after one step (i.e. how far one is removed from the stable gait pattern, c.f. [40]) than on the relative divergence rate, which is quantified by λ_S . It thus seems that the total amount of divergence after a given time may provide more valuable information on the stability of the gait pattern. Future studies could test this explanation and provide more information on the optimal time interval over which to determine divergence.

However, this may pan out, the fact that the $\log(\text{distance between initial nearest neighbours after 50 samples})$ (and to a lesser extent λ_S) correlated well with global stability over a range of different manipulations, renders this measure as a viable starting point for assessing stability in human gait.

4.2. Relationship between λ_L and probability of falling

The relationship between λ_L and actual stability (as expressed by the maximum allowable perturbation) found in the current study was either very weak (i.e. low correlation coefficients), or opposite to the expected relationship, as higher values of λ_L coincided with better stability. Interestingly, in some of the literature in which λ_L was used, the reported effects were also opposite to the expected effects. For instance, Dingwell et al. [9,11], Manor et al. [21] and Fallah Yakhdani et al. [6] reported that patient groups (diabetic neuropathy, peripheral neuropathy and knee osteoarthritis patients, respectively) had a lower λ_L compared to their healthy

controls. Moreover, in studies in which stability was experimentally impaired, by either Galvanic Vestibular Simulation [27], by having subjects walk on a compliant surface [26], or by applying visual or mechanical perturbations [28], impaired stability led to lower values of λ_L . In most of these studies, the lower λ_L was regarded as a sign of “adaptation” to instability; patients would somehow know they are more likely to fall, and adopt a more stable strategy. However, in some studies [6,13–15], the effects of walking speed on λ_S and λ_L were reported to be opposite, which can only be explained by assuming that these adaptations only occurred over longer time scales. The results of the current study suggest that an increased λ_L does not reflect an “adaptation”; the model used is fully passive, and possessed no adaptive properties. Still, even with fully passive dynamics, the increase in λ_L seemed, at least for some manipulations, to coincide with an increase in stability as indicated by an increase in the maximum perturbation the model could handle. A possible explanation could be that the maximum divergence that can be reached is limited by the attractor size [28]. Therefore, as long as the model keeps walking and divergence is initially fast, divergence should be slower later on. Nonetheless, this does not agree with the apparent absence of saturation effects (i.e. the manipulations with higher values of $\log(\text{distance between neighbours at 400 samples})$ did not diverge less). A post hoc correlation between values of λ_L and λ_S , yielded correlation coefficients between -0.9 ($P < 0.001$) and -0.1 ($P = 0.6$) for the different manipulations, further supporting absence of saturation effects in at least some of the manipulations. Moreover, if saturation effects would cause increased λ_L values coinciding with higher stability, one would expect this relationship to hold for all manipulations. However, for some of the manipulations, there seemed to be no clear relationship between λ_L and global stability. Why this is so, remains unclear. Still, it is clear that, even in the most simplified model of human walking, λ_L is not related to global stability, which makes it very unlikely that it will be related to global stability in the even more complex case of human walking.

4.3. Limitations of the current study

The current study has some limitations that should be acknowledged. Like most modeling studies, it is unclear how well our findings may be generalized to other types of models, perturbations, or humans. Still, it should be noted that our findings are in agreement with findings in at least one very different model, namely a 3D passive dynamic walker [32]. Moreover, they are in agreement with studies using other types of perturbations to determine the maximum perturbation the model could handle [31], and when studying the use of these perturbations (the maximum horizontal force that can be applied at the hip) we found that this correlated well with λ_S (results not reported). Finally, our findings are in agreement with several studies on human gait [26–28,41] suggesting that they generalize to humans, at least a degree.

4.4. Local vs. global stability, and the probability of falling in humans

The local dynamic stability measures used in the present study reflect that the gait pattern was locally unstable, a finding that was also reported in previous studies on models as well as actual human gait [29,31,32,42–44]. At the same time, we know from literature that the pattern is orbitally (i.e. on a cycle to cycle, stroboscopic basis) stable [30]. It should be kept in mind, however, that we calculated only the largest Lyapunov exponent, and not the entire spectrum of Lyapunov exponents. For a conservative system (like our model), the sum of the spectrum should be < 0 , while there may be individual exponents that are > 0 .

Interestingly, several studies have been published to date (including the present one) which show that local instability correlates with global stability (the probability of falling) in a simple passive dynamic walking model [29,31], while for orbital stability, no such relationship could be confirmed [29,36,45]. Since measures of local dynamic stability and orbital stability are both measures of local stability (i.e. the stability of the model in the vicinity of the steady state solution), there should be another factor that differs between these measures. The most obvious difference is that orbital stability “ignores” the growth of perturbations tangential to the trajectory, and is thus not concerned with phase shifts, whereas local dynamic stability takes into account the growth of perturbations tangential to the trajectory [42]. This may also be the reason why both λ_S and λ_L show values >0 even though the model could still walk. While it could be tested whether tested λ_S and λ_L indeed reflect growth of perturbations tangential to the trajectory for our model, this would require rather elaborate mathematical analysis, which is beyond the scope of the current paper. However, for a similar model, it has been shown that the unstable eigenvector is partially tangential to the trajectory [42]. However, the growth of perturbations along the trajectory does not make the model leave its basin of attraction (it would merely cause a phase shift along the trajectory, with no movement orthogonal to the trajectory). Therefore, it is unlikely that this factor caused the difference between measures of local dynamic and orbital stability. The second difference between local dynamic stability and orbital stability is that orbital stability gives only an indication of the entire gait cycle. In fact, it has been shown that orbital stability of a simple dynamic walker results from interactions of regions in the gait cycle that are locally unstable, and regions that are locally stable [42]. For λ_L , it seems unlikely that these tendencies of regions play a role, as it pertains to behaviour over many gait cycles. However, λ_S could well be strongly influenced by these fluctuations of stability in different regions of the gait cycle, which may be another reason why $\lambda_S > 0$. Future research should incorporate this idea to investigate whether it is the local instabilities-, or the local stabilities-, along the gait cycle that are important in determining the probability of falling.

While λ_S predicted probability of falling fairly well in the present study, it must be kept in mind that our model was entirely passive, and could not exert control. In humans, it may well be that the ongoing steady state gait pattern, although controlled, can be described in similar terms. Still, when this pattern is compromised, humans likely employ some kind of recovery strategy [46]. The probability of falling will thus not only depend on their steady-state gait stability, but also on the quality of those recovery actions, which is not necessarily correlated with the stability of the gait pattern [46].

5. Conclusions

The current study shows that, in a passive dynamic walking model, λ_S correlates with global stability, although this relationship was dependent on changes in the distance between initial nearest neighbours. A measure independent of such changes (the $\log(\text{distance between initially nearest neighbours after 50 samples})$) correlated well, and caused a similar relationship with global stability between manipulations. λ_L showed either weak correlations, or correlations opposite to expected, with higher values of λ_L coinciding with better stability, which questions the use of this measure as a predictor of global gait stability.

Acknowledgement

This work was partly funded by a grant from Biomet Nederland.

Conflict of interest statement

None of the authors of this paper have any financial and personal relationships with other people or organizations that could inappropriately influence the presented work.

References

- [1] Rubenstein LZ. Falls in older people: epidemiology, risk factors and strategies for prevention. *Age Ageing* 2006;35(Suppl. 2):ii37–41.
- [2] Lockhart TE, Liu J. Differentiating fall-prone and healthy adults using local dynamic stability. *Ergonomics* 2008;51(12):1860–72.
- [3] Kang HG, Dingwell JB. Effects of walking speed: strength and range of motion on gait stability in healthy older adults. *J Biomech* 2008;41(14):2899–905.
- [4] Kang HG, Dingwell JB. Dynamic stability of superior vs. inferior segments during walking in young and older adults. *Gait Posture* 2009;30(2):260–3.
- [5] Kang HG, Dingwell JB. Dynamics and stability of muscle activations during walking in healthy young and older adults. *J Biomech* 2009;42(14):2231–7.
- [6] Fallah Yakhani HR, Abbasi Bafghi H, Meijer OG, Bruijn SM, van den Dikkenburg N, Stibbe AB, et al. Stability and variability of gait in knee osteoarthritis before and after replacement surgery. *Clin Biomech* 2010;25(3):230–6.
- [7] Moraiti C, Stergiou N, Ristanis S, Georgoulis AD. ACL deficiency affects stride-to-stride variability as measured using nonlinear methodology. *Knee Surg Sports Traumatol Arthrosc* 2007;15(12):1406–13.
- [8] Dingwell JB, Kang HG, Marin LC. The effects of sensory loss and walking speed on the orbital dynamic stability of human walking. *J Biomech* 2007;40(8):1723–30.
- [9] Dingwell JB, Cusumano JP, Sternad D, Cavanagh PR. Slower speeds in patients with diabetic neuropathy lead to improved local dynamic stability of continuous overground walking. *J Biomech* 2000;33(10):1269–77.
- [10] Lamoth CJ, Ainsworth E, Polonski W, Houdijk H. Variability and stability analysis of walking of transfemoral amputees. *Med Eng Phys* 2010;32(9):1009–14.
- [11] Dingwell JB, Cusumano JP. Nonlinear time series analysis of normal and pathological human walking. *Chaos* 2000;10(4):848–63.
- [12] Rosenstein MT, Collins JJ, Deluca CJ. A Practical Method for Calculating Largest Lyapunov Exponents from Small Data Sets. *Physica D* 1993;65(1–2):117–34.
- [13] Bruijn SM, Ten Kate WRT, Faber GS, Meijer OG, Beek PJ, Dieën JH. Estimating dynamic gait stability using data from non-aligned inertial sensors. *Ann Biomed Eng* 2010;38(8):2588–93.
- [14] Bruijn SM, van Dieën JH, Meijer OG, Beek PJ. Statistical precision and sensitivity of measures of dynamic gait stability. *J Neurosci Methods* 2009;178(2):327–33.
- [15] Bruijn SM, van Dieën JH, Meijer OG, Beek PJ. Is slow walking more stable? *J Biomech* 2009;42(10):1506–12.
- [16] Dingwell JB, Marin LC. Kinematic variability and local dynamic stability of upper body motions when walking at different speeds. *J Biomech* 2006;39(3):444–52.
- [17] Manor B, Li L. Characteristics of functional gait among people with and without peripheral neuropathy. *Gait Posture* 2009;30(2):253–6.
- [18] Segal AD, Orendurff MS, Czerniecki JM, Shofer JB, Klute GK. Local dynamic stability in turning and straight-line gait. *J Biomech* 2008;41(7):1486–93.
- [19] Buzzi UH, Stergiou N, Kurz MJ, Hageman PA, Heidel J. Nonlinear dynamics indicates aging affects variability during gait. *Clin Biomech (Bristol, Avon)* 2003;18(5):435–43.
- [20] Stergiou N, Moraiti C, Giakas G, Ristanis S, Georgoulis AD. The effect of the walking speed on the stability of the anterior cruciate ligament deficient knee. *Clin Biomech (Bristol, Avon)* 2004;19(9):957–63.
- [21] Manor B, Wolenski P, Li L. Faster walking speeds increase local instability among people with peripheral neuropathy. *J Biomech* 2008;41(13):2787–92.
- [22] Kyvelidou A, Kurz M, Ehlers J, Stergiou N. Aging and partial body weight support affects gait variability. *J Neuroeng Rehab* 2008;5(1):22.
- [23] Dingwell JB, Cusumano JP, Cavanagh PR, Sternad D. Local dynamic stability versus kinematic variability of continuous overground and treadmill walking. *J Biomech Eng* 2001;123(1):27–32.
- [24] Hof AL, van Bockel RM, Schoppen T, Postema K. Control of lateral balance in walking: experimental findings in normal subjects and above-knee amputees. *Gait Posture* 2007;25(2):250–8.
- [25] Dean JC, Alexander NB, Kuo AD. The effect of lateral stabilization on walking in young and old adults. *IEEE Trans Biomed Eng* 2007;54(11):1919–26.
- [26] Chang MD, Sejdin E, Wright V, Chau T. Measures of dynamic stability: detecting differences between walking overground and on a compliant surface. *Hum Mov Sci* 2010;29(6):977–86.
- [27] Van Schooten KS, Sloot LH, Bruijn SM, Kingma H, Meijer OG, Pijnappels M, et al. Assessing gait stability: the sensitivity of trunk kinematics to galvanic vestibular stimulation. *Gait Posture* 2011;33(4):656–60.
- [28] McAndrew PM, Wilken JM, Dingwell JB. Dynamic stability of human walking in visually and mechanically destabilizing environments. *J Biomech* 2011;44(4):644–9.
- [29] Su JLS, Dingwell JB. Dynamic stability of passive dynamic walking on an irregular surface. *J Biomech Eng* 2007;129(6):802–10.
- [30] Garcia M, Chatterjee A, Ruina A, Coleman M. The simplest walking model: stability, complexity, and scaling. *J Biomed Eng-Trans ASME* 1998;120(2):281–8.
- [31] Kurz MJ, Markopoulou K, Stergiou N. Attractor divergence as a metric for assessing walking balance. *Nonlinear Dynam Psychol Life Sci* 2010;14(2):151–64.

- [32] Roos PE, Dingwell JB. Influence of simulated neuromuscular noise on the dynamic stability and fall risk of a 3D dynamic walking model. *J Biomech* 2011;44(8):1514–20.
- [33] Pijnappels M, Van der Burg JCE, Reeves ND, van Dieën JH. Identification of elderly fallers by muscle strength measures. *Eur J Appl Physiol* 2008;102(5):585–92.
- [34] Wu WH, Meijer OG, Bruijn SM, Hu H, van Dieën JH, Lamoth CJC, et al. Gait in pregnancy-related pelvic girdle pain: amplitudes, timing, and coordination of horizontal trunk rotations. *Eur Spine J* 2008;17(9):1160–9.
- [35] Huang Y, Bruijn SM, Lin J, Meijer OG, Wu W, Abbasi Bafghi H, et al. Gait adaptations in mild symptomatic lumbar disc herniation (LDH): trunk coordination and arm swing. *Eur Spine J* 2011;20(3):491–9.
- [36] Hobbelen DGE, Wisse M. A disturbance rejection measure for limit cycle walkers: the gait sensitivity norm. *IEEE Trans Robot* 2007;23(6):1213–24.
- [37] McGeer T. Passive dynamic walking. *Int J Robot Res* 1990;9(2):62–82.
- [38] England SA, Granata KP. The influence of gait speed on local dynamic stability of walking. *Gait Posture* 2007;25(2):172–8.
- [39] Zeng X, Eykholt R, Pielke RA. Estimating the Lyapunov-exponent spectrum from short time series of low precision. *Phys Rev Lett* 1991;66(25):3229–32.
- [40] Karssen JGD, Wisse M. Fall detection in walking robots by multi-way principal component analysis. *Robotica* 2009;27:249–57.
- [41] Sloom LH, Van Schooten KS, Bruijn SM, Kingma H, Pijnappels M, van Dieën JH. Sensitivity of local dynamic stability of over-ground walking to balance impairment due to galvanic vestibular stimulation. *Ann Biomed Eng* 2011;39(5):1563–9.
- [42] Norris JA, Marsh AP, Granata KP, Ross SD. Revisiting the stability of 2D passive biped walking: local behavior. *Phys D: Nonlinear Phenom* 2008;237(23):3038–45.
- [43] Kurz MJ, Judkins TN, Arellano C, Scott-Pandorf M. A passive dynamic walking robot that has a deterministic nonlinear gait. *J Biomech* 2008;41(6):1310–6.
- [44] Kurz MJ, Judkins T, Scott-Pandorf M, Arellano C. Can passive dynamic walking robots provide insights on nonlinear gait dynamics? *J Sport Exerc Psychol* 2007;29:S102–3.
- [45] Schwab AL, Wisse M. Basin of attraction of the simplest walking model. In: *Proc ASME Des Eng Tech Conf* 2001. 2001.
- [46] Bruijn SM, Beek PJ, Meijer OG, Dieën JH. The effects of arm swing on human gait stability. *J Exp Biol* 2010;213(Pt. 23):3945–52.